Microstructure development and high tensile properties of He/H2 milled oxide dispersion strengthened copper

Microstructure development and high tensile properties of He/H_2 milled oxide dispersion strengthened copper

S. M. S. Aghamiri[1,*] , N. Oono[1], S. Ukai[1], R. Kasada[2], H. Noto[3], Y. Hishinuma[3], T. Muroga[3]

[1]Graduate School of Engineering, Hokkaido University, Sappor 060-8628, Japan

[2] Institute of Materials Research, Tohoku University, sendai 980-8577, Japan

[3]National Institute of Fusion Science, Gifu 509-5202, Japan

Abstract

This study describes the effect of microstructural development on high tensile properties of a newly developed He/H_2 milled oxide dispersion strengthened copper in a large centimeter sized spherical morphology. Electron back scattered diffraction showed development of a strong texture of (110) plane in micron sized (1.2 μm) grains on the surface of milled spheres. A combination of microstructural features of inhomogeneous grain size, nanoscale lenticular/rectangular deformation twins, high dislocation density and fine oxide particles distribution induced a very high ultimate tensile strength (688 MPa)-ductility (8.6% elongation).

Keywords: Milled Cu-ODS; Texture; Tensile properties; Strengthening mechanisms

1. Introduction

Oxide dispersion strengthened (ODS) copper alloys are effective category of high heat flux materials for high temperature-irradiated environments due to presence of fine oxide particles [1]. The main processing route of commercially developed dispersion strengthened copper alloys such as Glidcop have been based on internal oxidation method for dispersion of alumina particles. However, high energy mechanical milling has been proved to possess a high potential in extensive development of different types of ODS materials especially ODS steels [2-4]. During ball milling of metallic powder, some development happens in the morphology, structure and properties of powder particles. Huang et al. [5] studied the effect of ball milling on pure copper powders and observed

* Corresponding author. Hokkaido University, Sappor 060-8628, Japan.

Email Address: sms.aghamiri@gmail.com

formation of large spheres of 2-2.5 mm diameters due to cold welding leaving large pores and some curved voids. In addition to important role of dislocation slip in the deformation process, they stated deformation of ball-milled copper proceeds by $[112]\ (11\bar{1})$ twinning and subgrains tend to form in the twins. Chawake et al. [6] investigated the evolution of morphology and texture during high energy milling of Ni and Ni-Cu powders. They observed development of $\{001\}$ texture in flaky morphology of powder particles which was attributed to extensive twinning in milled particles and a random texture developed via fragmentation into tiny particles during further milling. Generally, two types of deformation texture can develop during plastic deformation of fcc materials: copper-type texture in medium to high stacking fault energy alloys and Brass-type texture in low SFE ones [7]. It has been mentioned that copper-type texture is achieved by homogenous deformation of material by mechanism of slip of perfect dislocations while Brass-type texture originates from deformation twinning. Recently, some other deformation mechanisms of shear bands at special angles to rolling plane [8,9], partial slip of Shockley dislocations with $^{a}/_{6}\langle 112\rangle$ burgers vectors [10] and contribution of grain boundary sliding [11] have been proposed by different researchers for developing of Brass-type texture.

Experiences of high energy milling of fcc-structure metals have revealed that soft ductile powder particles agglomerate severely and attach to the milling medium and thus, prevent a homogenous distribution of oxide particles in the metallic matrix. During recent years, different approaches have been applied to prevent the agglomeration of soft copper particle. Cryomilling and process control agents have been used as effective methods against agglomeration [12-14]. In addition, hydrogen atmosphere has reported to embrittle the material and make a loose powder after milling [15-17]. In this work, we will investigate the effect of hydrogen containing atmosphere (He/5%H_2) on the powder morphology and microstructure development of the ODS copper alloy (Cu-ODS) and subsequent tensile properties are compared to previous processed copper alloys.

2. Experimental

In this study, Cu-ODS with a nominal composition of Cu-0.5wt% Y_2O_3 was prepared by using high energy milling. A high purity (99.9%) copper powder with the mean particle size of 50 μm and Y_2O_3 nanopowder with the mean particle size of 50 nm were used as raw materials. The powder mixture was mechanically milled using Fritch-P6 planetary ball mill in He/5 vol%H_2 gas atmosphere. The ball milling was performed for 48 hours with ball to powder ratio of 10:1 and different rotation speeds up to 470 rpm.

X-ray diffraction was conducted by means of $Cu - K_\alpha$ radiation with a Philips X´Pert PRO to specify the milled copper peaks. In addition, the specimen was observed by electron backscatter diffraction (EBSD) equipment attached to a field emission scanning electron microscope (JEOL JSM-6500F) operating at 15 kV with a step size of 20 nm. The observations were made on the surface of milled particles after cutting and flattening the sphere particles with a light roll. Sample preparation for EBSD was done by grinding with SiC paper up to 2000 grit and then polishing with 1 μm diamond paste and final polishing with Struers colloidal silica suspension. To attain EBSD data, TSL-OIM software was used for different analyses of inverse pole figure (IPF) and grain boundary map, orientation distribution function (ODF) at $\varphi_2 = 0°$ and grain size measurements. A 200 kV-JEOL JEM-2010 transmission electron microscope (TEM) and 300 kV-FEI-Titan scanning transmission electron microscope were used to study the microstructure of milled sample in high magnification. The thin foil for TEM observation was prepared by focused ion beam (FIB) (JEOL JIB-4600F) and the thinning was accomplished up to the thickness of ~100nm.

Vickers microhardness data of different milled samples were obtained by a HMV-Micro Hardness Tester-SHIMADZU, under a load of 980 mN with a dwell time of 30 s with 10 times measurements. The average Vickers microhardness was reported, and the maximum and minimum values were shown as error bar. In order to evaluate mechanical properties, uniaxial tensile tests were performed at ambient temperature under a strain rate of 1.0×10^{-3} s^{-1} using Shimadzu, SSL-1KN tensile machine. Three miniaturized size specimens were prepared using an electro-discharge processing machine and tested with a gauge dimension of 5 mm in length, 1.2 mm in width and 0.5 mm in thickness.

3. Results and discussion

3.1. Morphology and composition of milled powder

Fig. 1 shows the milled Cu-ODS after ball milling for 48 h at rotation speed of 470 rpm. An unexpected morphology of hollow spherical shaped particles with a large size up to 15 mm and a wall thickness of 0.6 mm can be observed in the figure. This morphology suggests that copper powder particles still have a considerably ductile behavior in hydrogen containing atmosphere, which is in contrary to previous report of Eckert at al. [15]. This result also has a contrast to brittle behavior of ODS Ferritic steel powder during milling in H_2 [17]. The chemical composition of milled Cu-ODS in Table. 1 indicates that 0.44 wt% yttria oxide particles dispersed in the copper matrix and a high amount of 2 wt% iron impurity in addition to other elements of Cr, C and O are in the composition. The existence of iron and Cr are attributed to the wear of milling medium and balls during ball milling of powders probably due to embrittlement by hydrogen.

Fig. 2 shows the combinatorial diagram presenting change of Vickers microhardness (HV0.1) and sphere size versus different rotation speeds of 200, 300, 400 and 470 rpm. As observed in the diagram, Vickers microhardness is enhancing with increasing the rotation speed of milling from $182\pm9HV_{0.1}$ to $208\pm3HV_{0.1}$, and in parallel, the diameter of milled spheres is growing considerably from 0.8 mm in 200 rpm to 8 mm in 470 rpm as illustrated in related images. The horizontal axis of milling rotation speed is represented to equivalent milling energy based on the unit of gravity (G) used for planetary-type ball mills. The results clearly show that milling energy affected significantly on hardness (14% gain) and size (10 times) of the milled product.

3.2. Microstructure and texture development

The microstructural characterization of He/H_2 milled Cu-ODS at 470 rpm was studied by EBSD and X-ray diffraction in Fig. 3. Typical green grains with the average size of 1.2μm can be observed in the IPF map (Fig. 3(a)) which is much higher than the crystallite size in the milled powder-morphology Cu-ODS in the same condition [14]. Evaluation of the microstructure shows that some grain growth up to some tens of micrometers has been formed in specific areas. The related grain boundary map (Fig. 3(b))

reveals formation of some fine subgrains and division of some grains by low angle boundaries (LABs)(<15º) with an area fraction of about 40% of total boundaries, while some portions of LABs (as shown by arrow) are disappearing and coarsening of grains is in progress. The ODF at $\varphi_2 = 0°$ (Fig. 3(c))) indicates a strong tape of (011) plane named Brass-type texture has formed with a max. intensity of 25 times than random on the surface plane of milled spheres with the main orientations of Goss($\{011\}\langle 100\rangle$), Brass ($\{011\}\langle 2\bar{1}1\rangle$) and P ($\{011\}\langle 1\bar{2}2\rangle$). X-ray diffraction in Fig. 3 (d) confirms the strong texture of (110) plane as a high intensity of (220) peaks in comparison to very low intensity of other planes. Development of the micron sized Brass-type textured microstructure in the Cu-ODS during process of milling is a new interesting finding in textural studies.

TEM studies of He/H_2 milled Cu-ODS sample give more understanding of effective parameters on microstructural development in the following. Fig. 4(a) shows formation of a complex microstructure including inhomogeneous grain size such that some fine grains or subgrains of ~ 100 nm (shown by arrows) are decorated around the larger micron sized grains without clear grain boundaries. Dark contrast of the microstructure is indicative of high deformation stored during milling inside the whole area which result in high dislocation density as observed clearly in a few grains in Fig. 4(b). Fig. 4(c and d) show that two types of deformation twins have developed during severe plastic deformation of He/H_2 milled Cu-ODS: a considerable area fraction (~35%) of the sample is covered by rectangular morphology twins elongated with a typical size of 70nm×677nm (Fig. 4 (c)), and a colony of nanoscale twins with different type of lenticular morphology have been formed with specific orientation in the matrix (Fig. 4 (d)). The thickness of these deformation twins is less than 10 nm with a length of ~100 nm which are much smaller than similar twin/matrix lamellae during dynamic plastic deformation of copper [18]. The Brass-type texture may originate from the developed deformation twins as mentioned in the literature [7]. The other microstructural parameter as indicated in Fig. 4(e) is the fine distribution of Y_2O_3 oxide particles confirmed by EDS analysis. Based on the TEM observation, the average size of dispersed oxide particles is ~5 nm with an interparticle spacing of ~67 nm. Remaining of fine oxide particles in milled

copper matrix is in contrast to dissolution of oxide particle frequently observed during mechanical alloying of ODS iron-based alloys [2,19].

3.3. Mechanical properties and strengthening mechanisms

Fig. 5 shows the engineering tensile stress-strain curve of He/H_2 milled Cu-ODS in compared to annealed Cu-ODS [14]. As observed, A very high UTS of 688MPa together with a total elongation of 8.6% is obtained which is much higher than previously processed ductile copper alloys in cold worked or annealed condition [1,13,14]. In addition, the tensile curve expresses a 0.2% yield stress of 673MPa close to UTS value, indicating a low strain hardening capacity of the material before yielding due to prior high strain storage during milling process. To understand the contribution of different strengthening mechanisms on achieving high tensile strength, total strength (σ_t) was estimated based on the observed microstructural findings in the following:

$$\sigma_t=\sigma_{GB}+ \sigma_{TB} +\sigma_{Dis.} +\sigma_{ODS} \quad (1)$$

where, σ_{GB}, σ_{TB}, σ_{Dis} and σ_{ODS} are grain boundary, dislocation forest, twin boundary and oxide dispersion strengthening, respectively. The effect of grain boundary and twin boundary strengthening was calculated based on the Hall-Petch relation [14]:

$$\sigma_{HP} = \sigma_0 + K_{HP} d^{-1/2} \quad (2)$$

where σ_0 is Peierls stress (near zero for copper), and K_{HP} as Hall–Petch constant (4.5 $MPa.mm^{1/2}$). By considering a fraction of 35% twin formation in the sample according to TEM observations, with an average twin size used in [4] and grain size of 1.24 μm for remaining grains according to EBSD results, the sum of σ_{GB} (83MPa) and σ_{TB} (82MPa) is 165 MPa. Furthermore, the other strengthening based on dislocation accumulation can be calculated by following relation [20]:

$$\sigma_{Dis.}= \alpha M G b \rho^{1/2} \quad (3)$$

where α is a constant (0.5 [21]), M as Taylor factor (3.26 for Brass texture [22]), G is shear modulus (44.7 GPa), b is Burgers vector (0.255nm) [14] and ρ is dislocation density (estimated about $2.5*10^{14}$ from the hardness value of He/H_2 milled ($208HV_{0.1}$) in

compared to Ar-milled ($226HV_{0.1}$) condition). Based on these parameters, the strengthening by dislocation accumulation is estimated to be 294MPa. And the last contribution of oxide dispersion strengthening can be evaluated by the following relation [14]:

$$\sigma_{ODS} = 0.84\frac{MGb}{2\pi r\sqrt{1-\nu}(\sqrt{3\pi/2f}-\pi/4)}\ln(\frac{\pi r}{4b}) \quad (4)$$

considering M as Taylor factor, G as shear modulus and b as the Burgers vector with the same as previous values, r as the average radius of oxide particles (2.54nm) and f as the fraction of oxide particles (0.0079), σ_{ODS} is calculated to be 209MPa. So, the result of all evaluated strengthening contributions by grain size, twins, dislocation forest and fine oxide particle is about 668 MPa, a near value to 0.2% yield strength of He/H_2 milled Cu-ODS at 673MPa.

4. Conclusion

In summary, a new Cu-ODS was developed via high energy milling in $He/5\%H_2$ atmosphere with hollow spherical-shape particles up to 15mm diameter. EBSD analysis formation of a strong texture of (011) plane (Brass-type texture) with an average grain size of 1.2 μm. The microstructure development included an inhomogeneous grain size, a high fraction (35%) rectangular morphology twinning together with lenticular twins, a dislocation forest and dispersion of fine oxide particles with an average diameter of ~5nm and interparticle spacing of 67nm. The tensile properties including high UTS of 688MPa with a good ductility of 8.6% total elongation were achieved with the strengthening contributions of 44% dislocation strengthening, 31% oxide dispersion strengthening and 25% grain/twin boundaries.

Acknowledgement

This work is supported by Grant-in-Aid for Scientific Research(A), 16H02443, Japan Society for the Promotion of Science.

References

1-M. Li, S. J. Zinkle, Physical and Mechanical Properties of Copper and Copper Alloys, in: R.M.J. Konings (Eds.), Comprehensive Nuclear Materials, Vol. 4, Elsevier Ltd., 2012, 667-690.

2-S. Ukai, Oxide Dispersion Strengthened Steels, in: R.M.J. Konings (Eds.), Comprehensive Nuclear Materials, Vol. 4, Elsevier Ltd., 2012, pp. 241–271.

3-S.M. Seyyed Aghamiri, H.R. Shahverdi, S. Ukai, N. Oono, K. Taya, S. Miura, S. Hayashi, T. Okuda, Microstructural characterization of a new mechanically alloyed Ni-base ODS superalloy powder, Mater Charact 100 (2015) 135.

4-H. Yu, S. Ukai, N. Oono, Tensile properties of Co-based oxide dispersion strengthened superalloys, Journal of Alloys and Compounds 714 (2017) 715-724.

5-J.Y. Huang, Y.K. Wu, H.Q. Ye, Ball milling of ductile metals, Materials Science and Engineering A199 (1995) 165-172.

6-N. Chawake, R. S. Varanasi, B. Jaswanth, L. Pinto, S. Kashyap, N.T.B.N. Koundinya, A. K. Srivastav, A. Jain, M. Sundararaman, R. S. Kottada, Evolution of morphology and texture during high energy ball milling of Ni and Ni-5wt%Cu powders, Materials Characterization 120 (2016) 90–96.

7-T. Leffers, R. K. Ray, The brass-type texture and its deviation from the copper-type texture, Progress in Materials Science 54, 2009, 351–396

8-L. Lapeire, J. Sidor, P. Verleysen, K. Verbeken, I. De Graeve, H. Terryn, L.A.I. Kestens , Texture comparison between room temperature rolled and cryogenically rolled pure copper, Acta Materialia 95, 2015, 224–235.

9-E. El-danaf, S. R. Kalidindi, R. D. Doherty and C. Necker, Deformation Texture Transition in Brass: Critical Role of Micro-Scale Shear Bands, Acta Mater. 48 (2000) 2665–2673.

10-C.F. Gu, L.S. Toth, Y.D. Zhang and M. Hoffman, Unexpected brass-type texture in rolling of ultrafine-grained copper, Scri Mater 92, 2014, 51–54.

11-W. Skrotzki, A. Eschke, B. Jo´ni, T. Unga´r, L.S. To´th, Yu. Ivanisenko, L. Kurmanaeva, New experimental insight into the mechanisms of nanoplasticity, Acta Materialia 61, 2013, 7271–7284.

12-C. Suryanarayana, Mechanical alloying and milling, Progress in Materials Science 46 (2001) 1–184.

13-D.V. Kudashov, H. Baum, U. Martin, M. Heilmaier, H. Oettel, Microstructure and room temperature hardening of ultra-fine-grained oxide-dispersion strengthened copper prepared by cryomilling, Materials Science and Engineering A 387–389 (2004) 768–771.

14-S.M.S. Aghamiri, N. Oono, S. Ukai, R. Kasada, H. Noto, Y. Hishinuma, T. Muroga, Microstructure and mechanical properties of mechanically alloyed ODS copper alloy for fusion material application, Nuclear Materials and Energy 15 (2018) 17–22.

15-J. Eckert, J. C. Holezer, C. E. Krill and W. L. Johnson, Investigation of nanometer-sized FCC metals prepared by ball milling, Materials Science Forum, 88-90 (1992) pp 505-512.

16-Z. Oksiuta , N. Baluc, Effect of mechanical alloying atmosphere on the microstructure and Charpy impact properties of an ODS ferritic steel, Journal of Nuclear Materials 386–388 (2009) 426–429.

17-N. Y. Iwata, T. Liu, P. Dou, R. Kasada, A. Kimura, T. Okuda, M. Inoue, F. Abe, S. Ukai, S. Ohnuki, T. Fujisawa, Effects of MA environment on the mechanical and microstructural properties of ODS ferritic steels, Journal of Nuclear Materials 417 (2011) 162–165.

18- Y.S. Li, N.R. Tao, K. Lu, Microstructural evolution and nanostructure formation in copper during dynamic plastic deformation at cryogenic temperatures, Acta Materialia 56 (2008) 230–241.

19-Y. Kimura. S. takaki, S. Suejima, R. Uemori and H. Tamehir, Ultra Grain Refining and Decomposition of Deformation in Oxide Dispersion Ferritic Oxide during Super-heavy Stainless Steel Powder, ISIJ International, Vol. 39 (1 999), No. 2, pp. 176-182.

20-D. A. Hughes, N. Hansen, The microstructural origin of work hardening stages, Acta Materialia, 148 (2018) 374-383.

21-H.D. Chandler , Work hardening characteristics of copper from constant strain rate and stress relaxation testing, Materials Science and Engineering A 506 (2009) 130–134

22-S. Chang, D. Hou and Y. Chang, The effect of textures and grain shape on the shear band formation in rolled FCC metals, Acta metall. 37, 7, (1989) 2031-2033.

Figures

Tables

Fig. 1.

Wall thickness: ~0.6

Fig. 2.

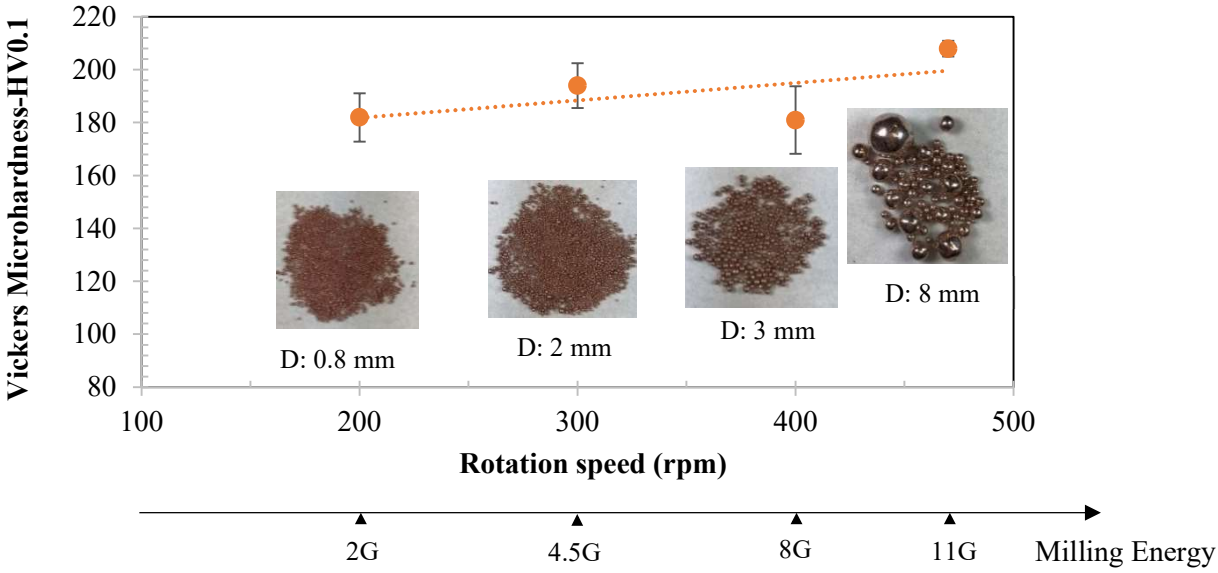
Vickers Microhardness-HV0.1
220
200
180
160
140
120
100
80
100
200
300
400
500
Rotation speed (rpm)
D: 0.8 mm
D: 2 mm
D: 3 mm
D: 8 mm
2G
4.5G
8G
11G
Milling Energy

Fig. 3.

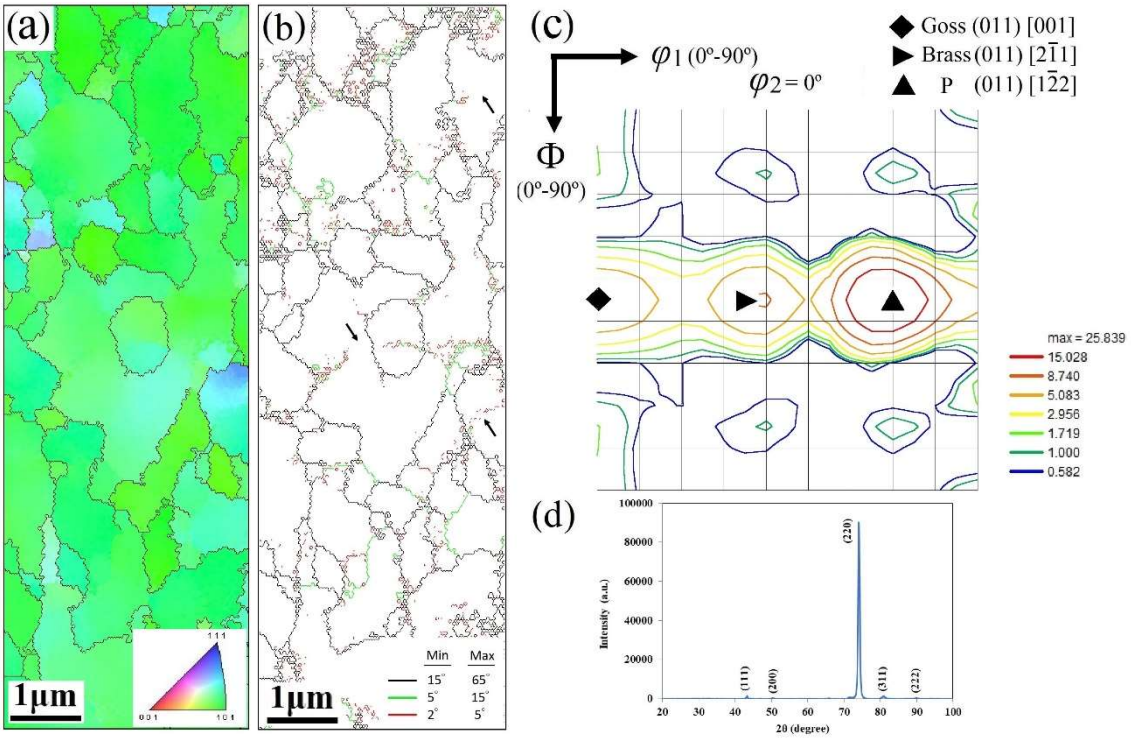
(a)
1µm
(b)
1µm
Min
Max
15°
65°
5°
15°
2°
5°
(c)
φ1 (0°-90°)
φ2 = 0°
Φ
(0°-90°)
Goss (011) [001]
Brass (011) [2$\bar{1}$1]
P (011) [1$\bar{2}$2]
max = 25.839
15.028
8.740
5.083
2.956
1.719
1.000
0.582
(d)
Intensity (a.u.)
2θ (degree)
(111)
(200)
(220)
(311)
(222)

Fig.4.

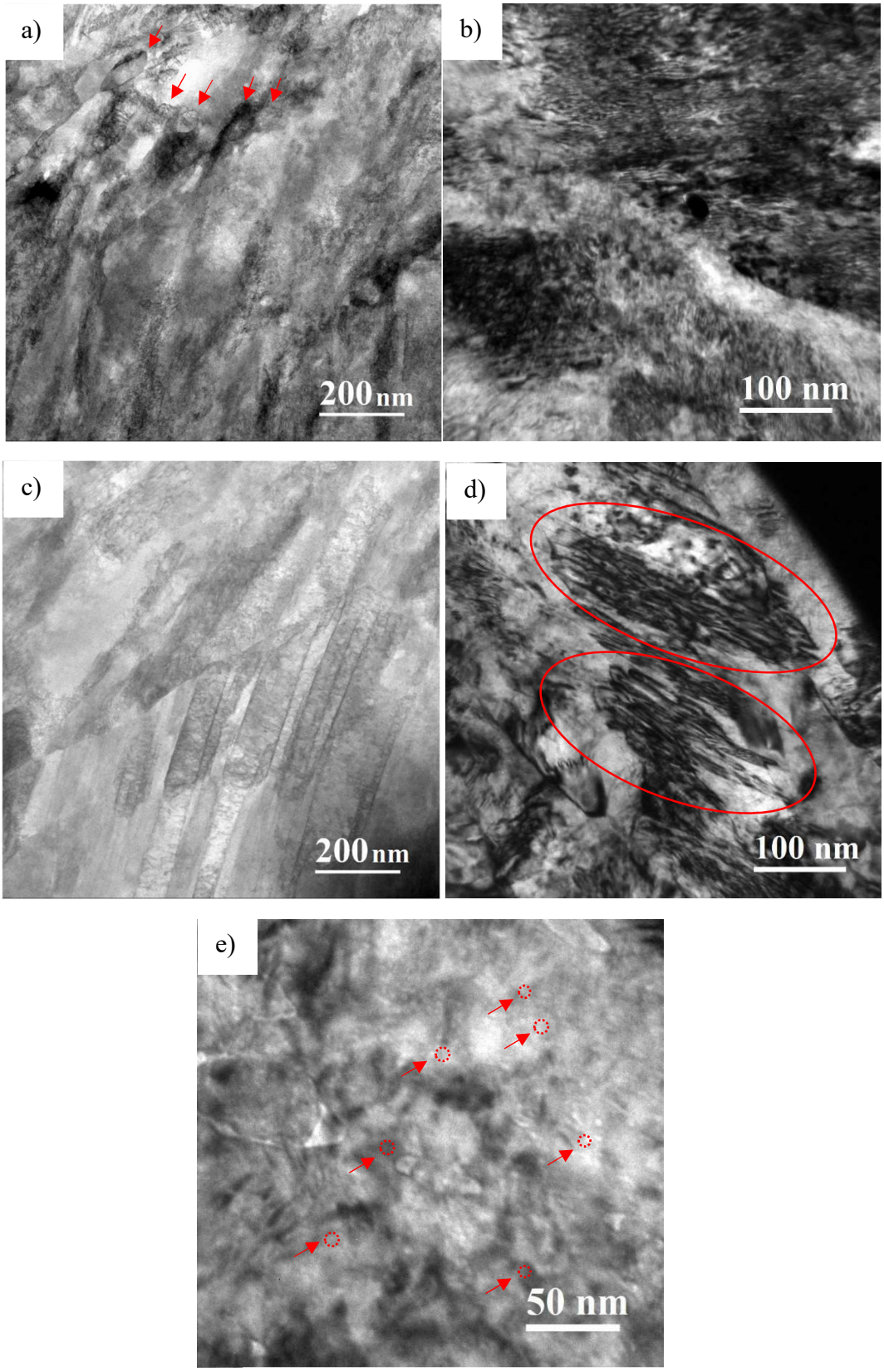

Fig. 5.

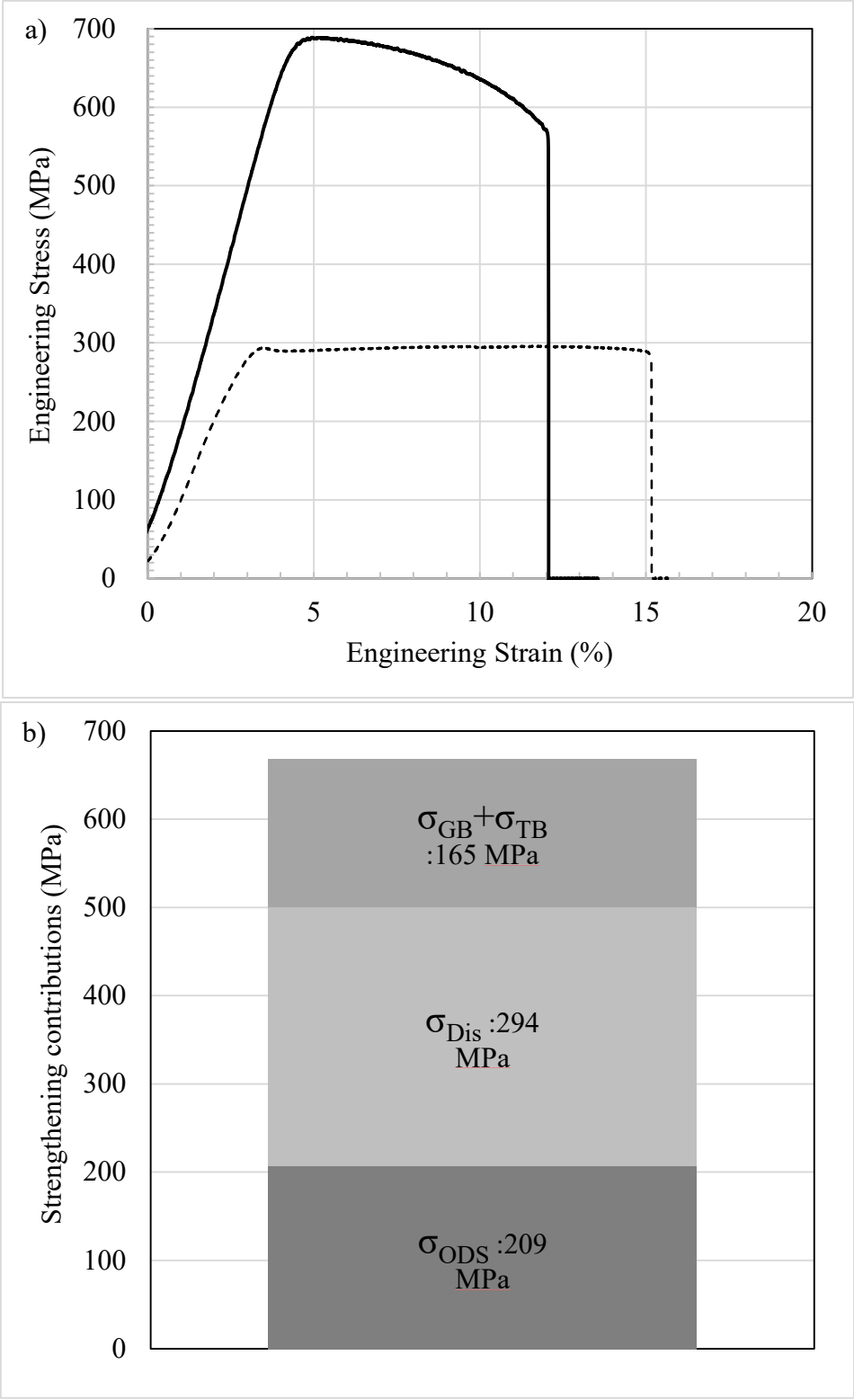
a)
Engineering Stress (MPa)
0
100
200
300
400
500
600
700
0
5
10
15
20
Engineering Strain (%)
b)
Strengthening contributions (MPa)
0
100
200
300
400
500
600
700
σGB+σTB
:165 MPa
σDis :294
MPa
σODS :209
MPa